CHAPTER 6

Comparative study of Mg based spinels like $MgCr_2O_4$ and MgV_2O_4 for glycerol carbonate synthesis

CHAPTER 6

6.1 Introduction

The rapid growth of population and technological development worldwide leads to continuous increase of energy demand. In order to fulfil the energy demand now-a- days biodiesel industries were developed at large scale. The production of biodiesel as an alternative to fossil fuel results in generation of crude glycerol (approximately 10 wt.% of the total product) which remains as a glut in market. The surplus glycerol mainly hampers the market competitiveness of biodiesel industries. Considering all these issues, recent research attention is directed towards the sustainable and economical conversion of crude glycerol to various value added products [176-179]. Among all the derivatives of glycerol , glycerol carbonate is quite attractive product due to its outstanding physicochemical properties like low-flammability, water solubility and high biodegradability [20,54]. In this chapter we have designed magnesium based solid base catalysts like MgV_2O_4, $MgCr_2O_4$ and applied them in transesterification of glycerol. However, it was interesting and challenging to incorporate magnesium with transition metals like vanadium oxide, chromium oxide in order to enhances the stability, catalytic activity and basic strength of MgO. Here, we have also attempted to explore the role of effect of transition metals like Cr and V on the activity of magnesium metal in glycerol transesterification. Here, a series of magnesium-based transition metal oxide (Cr and V,) catalyst were synthesized by co-precipitation route and used in glycerol carbonate synthesis. The reactions were individually observed, over all these catalysts and conversion percentage of glycerol was also well studied. The relationship between conversion of reactant species, selectivity and yield percentage of product, acidic and basic properties were systematically analysed. Many characterization techniques like XRD, TGA-DSC, FE-SEM, BET-Surface area and XPS spectra were performed to identify the physicochemical properties of designed catalyst and their effect on catalytic performance.

6.2 Synthesis of spinel catalyst

The spinels of magnesium with different transition metals like $MgCr_2O_4$, and MgV_2O_4, were synthesized via co-precipitation route at constant pH range of 8-10 using metal nitrate as precursors. First of all, required amount of magnesium nitrate was taken in a beaker and dissolved in specific amount of de-ionised water. In another beaker specific amount of chromium nitrate was taken and dissolved with de-ionised water. Both the solutions were mixed with each other and was stirred at 40°C (Mg:Cr molar ratio equal to 1:2 in the reaction mixture). During the reaction process, there was dropwise addition of ammonia solution (ammonium hydroxide) in order to maintain the pH 8-10 as well as to form precipitation. After formation of precipitate, the reaction mixture was also stirred for another 5h to enhance the selective growth of precipitate phase. Then, the product mixture was filtered, washed with hot water several times in order to remove any impurities. After that the solid sample was kept in an oven at 110°C overnight and then calcined at 900°C for 4h in a muffle furnace. Finally, the resultant product was collected from the furnace and crushed and sieved to get the fine powder form of catalyst. The obtained catalyst was stored and further used in transesterification of glycerol. Similarly, catalysts like MgV_2O_4, were also synthesized and tested in transesterification of glycerol.

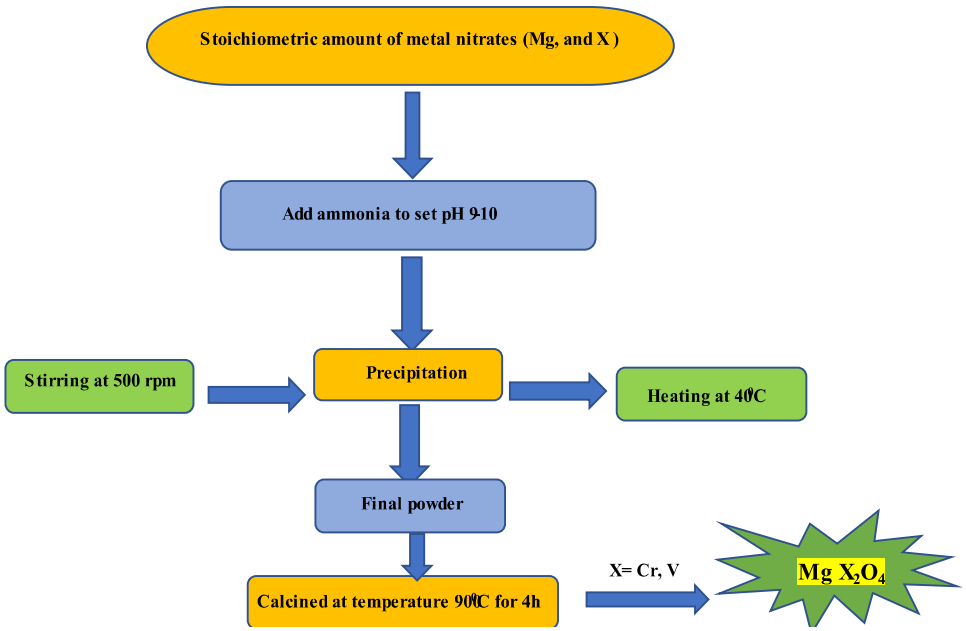

Scheme 6.1 Synthetic method for spinels like MCO and MVO via Co-precipitation route

6.3 Characterization of synthesized catalyst

6.3.1 TGA study

The thermal stability of synthesized spinels MCO and MVO were studied by thermogravimetric analysis under inert atmosphere. TGA plot of uncalcined MCO depicted in fig 6.1(a). There were three stages of mass decomposition occurred with rise in temperature. The first phase of weight loss happened around 100-220°C, which might be due to evaporation of surface adsorbed water molecules. The 2nd phase of mass loss occurred around 320- 475° C which could be due to release of crystal water, loss of capping agents or any organic moieties present in designed catalyst. From the graph, it was revealed that the 3rd stage of mass loss started around 490°C which is ascribed to disintegration of nitrate or carbonate species present in synthesized catalyst. The constant weight was reached around 800°C indicating the stable temperature of MCO spinel i.e., minimum

calcination temperature required for complete formation of $MgCr_2O_4$ catalyst. Similarly, TGA curve of MgV_2O_4 (MVO) is depicted in fig 6.1(b). In case of MVO, we obtained four phases of mass loss with subsequent rise in temperature. The first phase of mass loss had taken place around 100- 210°C which was attributed to evaporation of surface water. The 2nd phase of mass loss of the sample at 260-380°C which ascribed to removal of chemically adsorbed water molecules. The next phase (3rd) of weight loss happened at 530°C which might be due to removal of any organic or inorganic impurities. Around 600 to 800°C, it seems that there was also another phase of mass loss occurred which might be due to decomposition of nitrate or any other moieties and complete formation of mixed oxide. After 850°C the compound became stable indicating the appropriate calcination temperature of synthesized MVO [180-183].

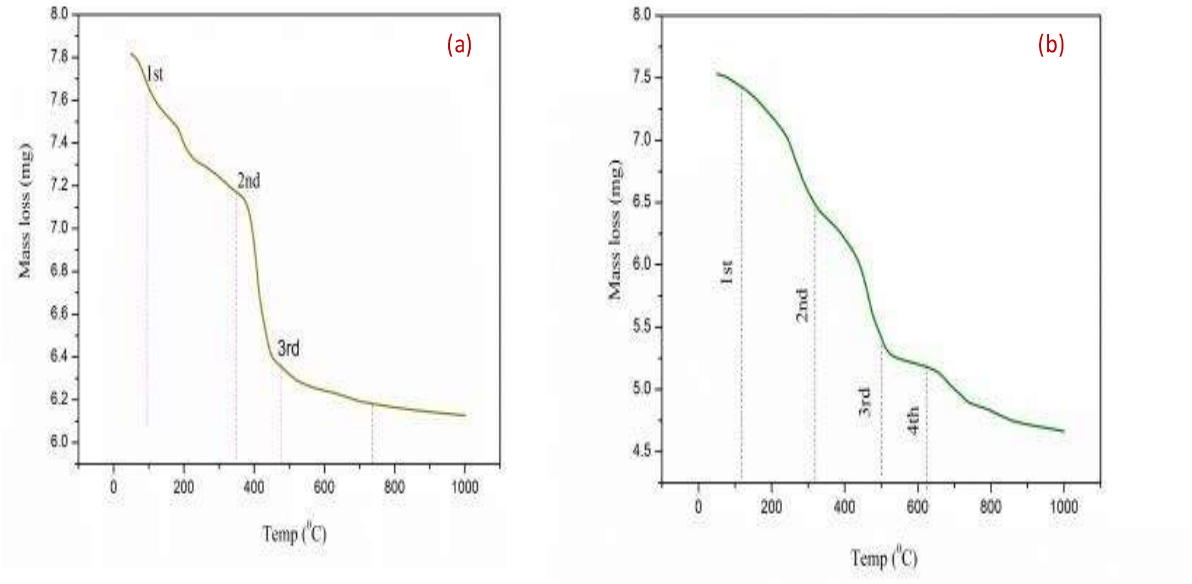

Fig 6. 1 TGA graph of uncalcined (a) $MgCr_2O_4$ (b) MgV_2O_4 spinels

6.3.2 XRD pattern

X-ray diffraction pattern being one of the reliable techniques for determination of crystalline structure, crystal orientation, crystallite size and phase of the compound was studied for both the synthesized catalysts. Fig 6. 2 (a) revealed the XRD pattern of MCO catalyst. It is seen that all the samples are cubic spinel type structure according to standard pattern of JCPDS file .The diffraction peaks at 2θ values 18.41°, 26.32°, 28.92°, 31.03°, 37.71°,43.40°,46.51°,51.43°,57.04°,60.08°,63.05°,66.28°,72.54°,75.62°,76.88°,79.64°and 87.52° can be indexed to miller indices (111), (211), (210), (222), (220), (311), (400), (420) ,(331), (422), (511), (440), (531), (620), (442), (444), (642) and (640) of crystal planes of spinel $MgCr_2O_4$ respectively, which matched with JCPDS No-100351. There were no other peaks in X-ray diffractogram of compound suggesting that single phase of $MgCr_2O_4$ crystal was formed and the very sharp and intensive peaks of $MgCr_2O_4$ confirmed the crystalline structure of catalyst [184–186] . Using Scherrer's equation from the diffraction peak (220), the crystallite size was calculated and found to be 34.6nm.

$$D = \frac{0.9\lambda}{\beta cos\theta} \qquad (6.1)$$

Where λ corresponds to wavelength of X-ray beam, β is the line broadening at full width at half maxima, D refers to average crystallite size and θ is the Bragg angle. The lattice parameter (a) and unit cell volume of $MgCr_2O_4$ catalyst were 9.36 A° and 578.4A^3 respectively.

Similarly in fig 6.2 (b), the major diffraction peaks at 2θ = 14.37°, 18.23°, 23.72°, 29.98°, 32.35°, 34.95°, 36.08°, 42.93°, 47.02°, 49.43°, 53.25°, 56.76°, 59.17°, 62.33°, 63.08°, 65.53°, 70.74°, 73.72°, 74.72°, 78.66°, 81.55° and 86.41° assigned to crystal planes of miller indices (100), (111), (211), (220), (310), (222), (300), (400), (331), (320), (411),(422), (511), (512), (440), (421), (531), (532), (622), (444), (551) and (642)

respectively. All the diffraction patterns were matched with JCPDS No - 772130 indicating a single crystal face centered cubic phase of MgV_2O_4 . The lattice parameter was calculated and found to be a = b = c = 8.27A°, and unit cell volume of MgV_2O_4 was obtained to be 482.76A^3. The average crystallite size of spinel MgV_2O_4 was calculated using above Scherrer equation and obtained to be 27.84nm. Comparing the XRD pattern of both $MgCr_2O_4$ and MgV_2O_4 spinel the diffraction peaks are more sharper and intensed in case of $MgCr_2O_4$ catalyst than that of MgV_2O_4 spinel indicating higher crystallinity in sample [185,187–189]. The higher crystallinity and higher lattice parameters of $MgCr_2O_4$ spinel might be one of reasons for better conversion of glycerol. The structural parameters and phase composition of both the spinels is represented in table 6. 1.

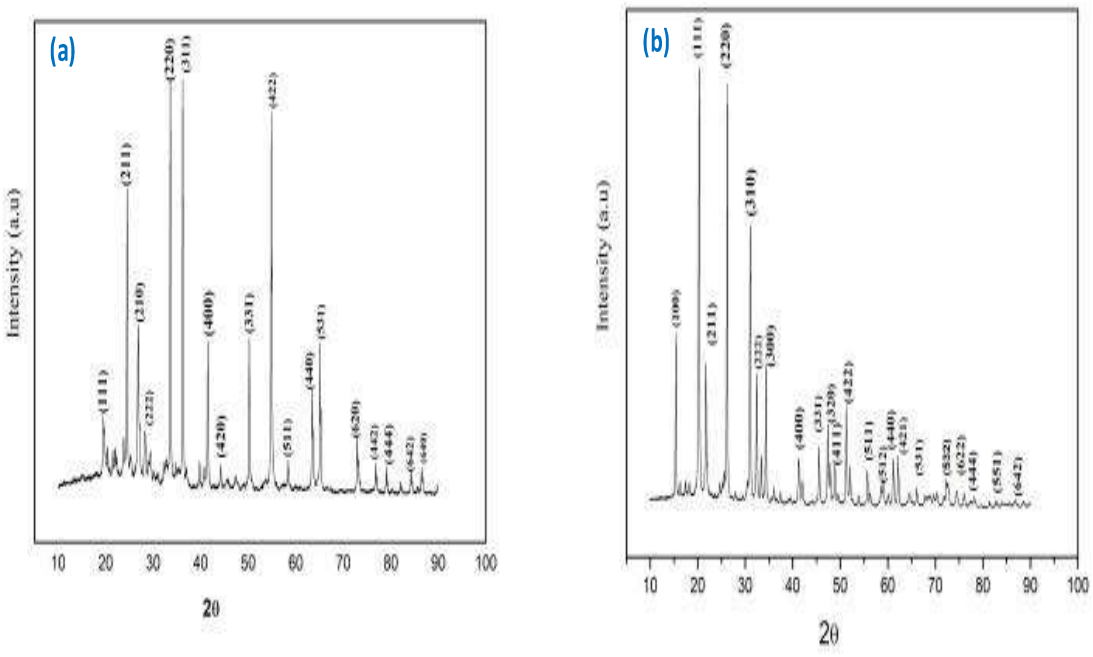

Fig 6. 2. XRD pattern of (a) $MgCr_2O_4$, (b) MgV_2O_4 calcined at 900°C

Table.6.1 Structural parameters and phase composition of synthesized spinels

Catalyst	Calcination temperature(°C)	Crystal phase	Lattice system	Lattice parameter (A°)	Unit cell volume ($A^{\circ 3}$)	Surface Area (m^2/g)	Pore volume (cm^3/g)	Pore diameter (nm)
$MgCr_2O_4$ (MCO)	900	Single phase	Cubic	9.36	578.4	28.7	0.074	18.6
MgV_2O_4 (MVO)	900	Single phase	Cubic	8.27	482.76	23.8	0.038	11.8

6.3.3 SEM-EDX study

The surface morphology and elemental composition of synthesized $MgCr_2O_4$ and MgV_2O_4 spinels were studied by SEM-EDX analysis. Fig 6.3 (b) depicted the SEM micrographs of $MgCr_2O_4$, it was observed that there was homogeneous distribution of intermixed grains of variable sizes having some porosity. The grains are finely distributed and signify the nano sized nature of $MgCr_2O_4$ spinel which exclusively enhanced the surface area of catalyst and was highly suitable for transesterification reaction of glycerol [190-191] . From elemental compositions and characteristics peak of magnesium chromite, energy line confirmed the elements like Mg, Cr and O are present with adequate amounts according to their atomic and weight percentage. Overall, EDX analysis confirmed the successful synthesis of $MgCr_2O_4$ catalyst. The SEM-EDX micrograph of MgV_2O_4 catalyst is shown in fig 6. 3 (a). It is revealed that the particles are not uniformly distributed in the microsphere of MgV_2O_4 catalyst. The particles possessed variable polyhedral shape of

uneven size i.e. non regular dimensional shape[192-193] . The particle size of MgV_2O_4 spinel is larger than that magnesium chromite although it is in nano range suggesting the decrease in surface area of magnesium vanadate (MVO) microsphere [194-195]. As a result, MVO has lesser activity in transesterification of glycerol than that of magnesium chromate (MCO). The elemental composition and intensity of peaks indicated in EDX histogram revealed that there was successful synthesis of MVO with respect to the atomic and weight percentage of elements like Mg, V and O present in the designed catalyst.

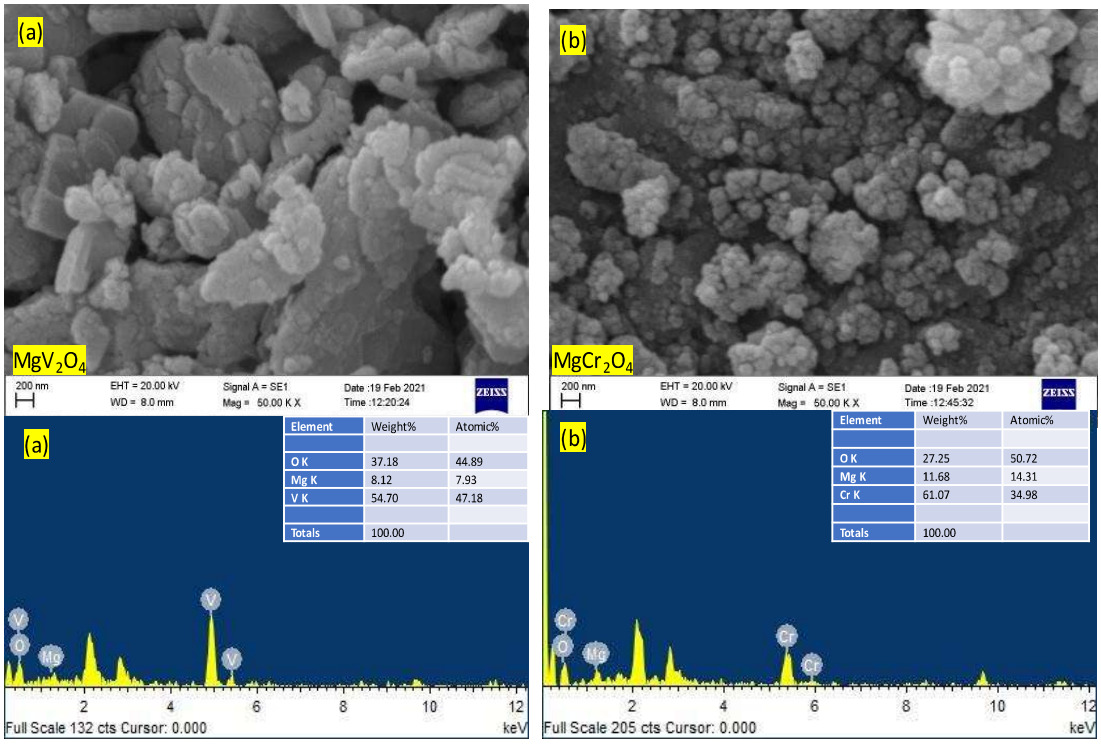

Fig 6. 3. SEM-EDX pattern of (a) MgV_2O_4, (b) $MgCr_2O_4$ spinels

6.3.4 BET surface area and Basicity study

The specific surface area, pore volume and pore diameter of the synthesized catalysts like MCO and MVO were determined through N_2 adsorption desorption isotherm and are depicted in fig 6. 4. The specific surface area of MVO was 23.8m^2/g where as the specific surface area of MCO was 28.7m^2/g which is larger than that of MVO. Similarly, the pore

size and pore volume distribution of MCO was higher as compared to that of MVO. The dimension of pores for MCO lies around 3.7- 18.6 nm whereas the pore size distribution of MVO lies in the range of 2.5- 11.8 nm respectively. Both the spinels having type IV hysteresis loop according to IUPAC classification and belong to mesoporous materials [186,196]. MCO having more concentrated pore size distribution and highest specific surface area facilitate the transesterification reaction of glycerol. As it is known that transesterification of glycerol in presence of heterogeneous catalyst is a surface phenomenon and catalytic activity prefers larger surface area so MCO catalyst having high surface area enhanced the conversion of glycerol than that of MVO catalyst [103,114].

The basic site and basicity of heterogeneous catalyst play major role in the transesterification of glycerol, as a result, it is highly required to study the basic strength and basicity of synthesized catalyst. Here, we studied all the properties by simple Hammett indicator titration method and the result obtained are represented in Table 6.2**.** The indicators like bromothymol blue (H_ =7.2), phenolphthalein (H_ = 9.8), 2,4- dinitroaniline (H_ = 15.0) , 4-nitroaniline (H_ = 18.4) were used in titration method. Around 25 mg of catalyst was taken and stirred with 1.0 cm^3 of Hammett indicator solution diluted with methanol and kept for 2h to equilibrate. After a certain time, there was change in colour of indicator solution implying the catalyst is a stronger base than indicator. The overall basicity of synthesized catalyst was quantitatively calculated by Hammett indicator benzene carboxylic acid titration method. It was observed that pure Mg $(NO_3)_2$ possessed H_ value in the range 9.8-15.0 which was relatively weak medium basic site to catalyst. Similarly, the parent Cr $(NO_3)_3$, $VO(NO_3)_3$ were being acidic by nature did not change the colour of bromothymol blue. The basic strength of all the salts were improved by addition of MgO. It was obtained that with addition of MgO the basic strength of catalysts came in the range of 15< H_ <18.4. Although, the basic strength of all the three catalysts were

similar but the number of basic sites (total basicity in terms of millimole /g) was highest for $MgCr_2O_4$ (MCO) in comparison to MgV_2O_4 (MVO) as given in table 6.1. MCO having highest basic site enhanced the conversion of glycerol as transesterification follows base catalysed reaction.

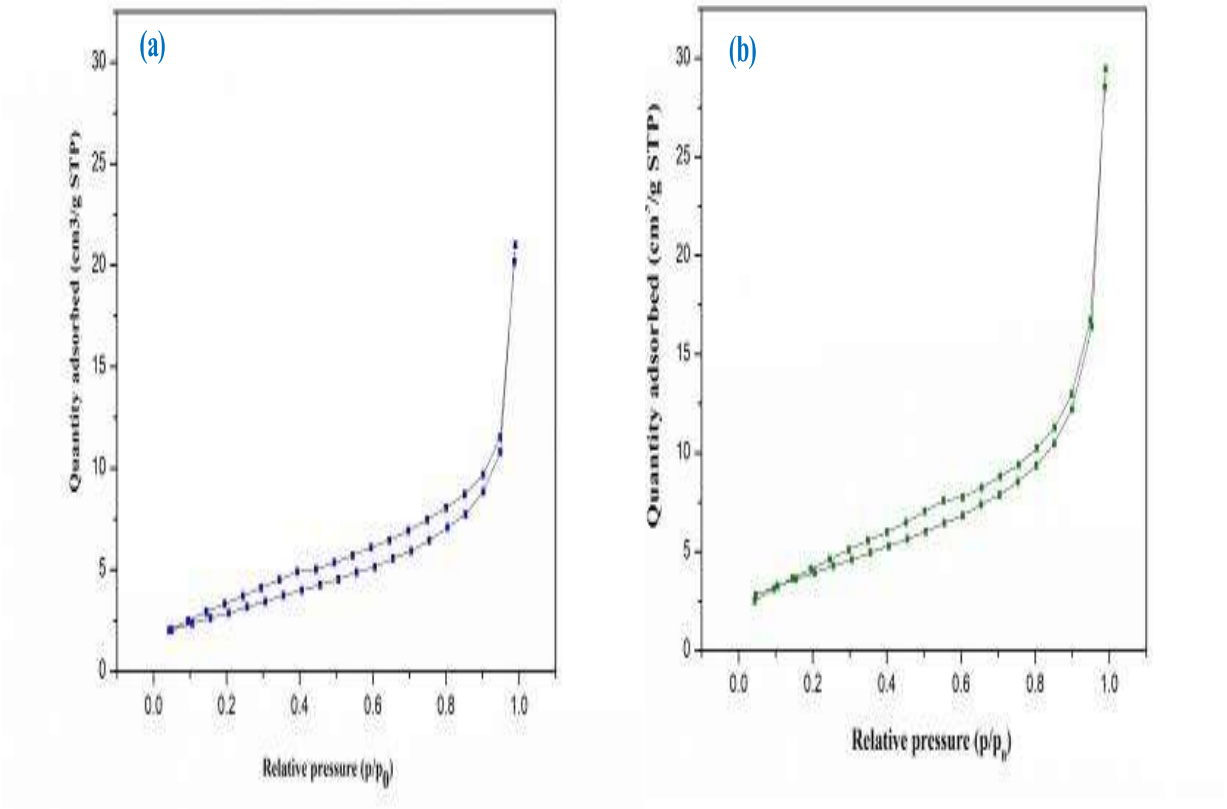

Fig 6. 4. BET-surface area of (a) MgV_2O_4, (b) $MgCr_2O_4$ spinels

Table 6.2. Basicity of Synthesized catalysts

Catalyst	Basic strength	Total basicity(mmolg^{-1})	Conversion (%)	Yield (%)
$Mg(NO_3)_2$	9.8-15.0	3.84	28	21
$VO(NO_3)_3$	9.8 -15.0	0.56	8.3	6.3
$Cr(NO_3)_4$	9.8 -15.0	0.31	5.7	2.98
MgV_2O_4	15.0 – 18.4	9.32	82.7	68
$MgCr_2O_4$	15.0 – 18.4	17.63	99.2	95.7

6.3.5 XPS spectra

The surface composition, chemical state and oxidation state of synthesized both spinels MCO and MVO were investigated by X-ray photoelectron spectroscopy (XPS) technique. The obtained results shown in fig 6.5, revealed that all the elements like Mg, Cr and O are present on the surface of catalysts. In case of MCO, chromium exhibits two types of oxidation state in Cr 2p region. The binding energy at 576.3eV corresponds to 2p $_{3/2}$ peak of Cr^{3+} species where as the binding energy at 579.0 eV assigned to 2p $_{3/2}$ of Cr^{6+} species [186,197] . The peak at 588.47eV corresponds to Cr $^{3+}$ $2p_{1/2}$. All these peaks are relatively nearer to standard binding energy Cr^{3+} of Cr_2O_3. Oxygen 1s spectra shows two distinguished deconvoluted peaks in two different binding energy states, such as the first binding energy at 530.06 eV attributed to lattice oxygen of metal oxygen bonding where as another peak at 532.64 eV arises may be due to oxygen vacancy or absorbed oxygen species in the form carbonates or hydroxyls [198-199]. Similarly, 1s spectrum of Mg is depicted in fig 6.5(b). The peak at binding energy 1304 eV corresponded to 1s spectra of Mg^{2+} species. The phenomena of surface composition and oxidation state of elements present in MVO spinel were explored by XPS survey and depicted in fig 6.6. The characteristic peak at 517.3eV assigned to $2P_{3/2}$ spectrum of Vanadium metal and the peak at 526.7eV correspond to V $2P_{1/2}$ spectrum. The difference in spin orbit coupling of core

level spectrum of V 2p spectrum was mostly about 7.4eV which confirmed that vanadium exists in +3 oxidation states [187–189]. Mg 1s shows the characteristics peak of Mg^{2+} at 1305.3eV. In O 1s spectrum the deconvoluted peaks at 529.6eV and 532.3eV assigned to bonded oxygen and oxygen defects in the sample respectively. The distribution of two different oxygen species can be measured by taking the ratio of [O_{ads}] / [O_{lat}] , higher area ratio indicates larger amount of oxygen vacancies whereas lower area ratio indicates lesser oxygen vacancies [190,199]. Here the area ratio of [O_{ads}] /[O_{Lat}] for MCO is bigger than that of MVO, hence MCO has higher amount of surface oxygen as well as vacant oxygen than that of MVO [200-202].

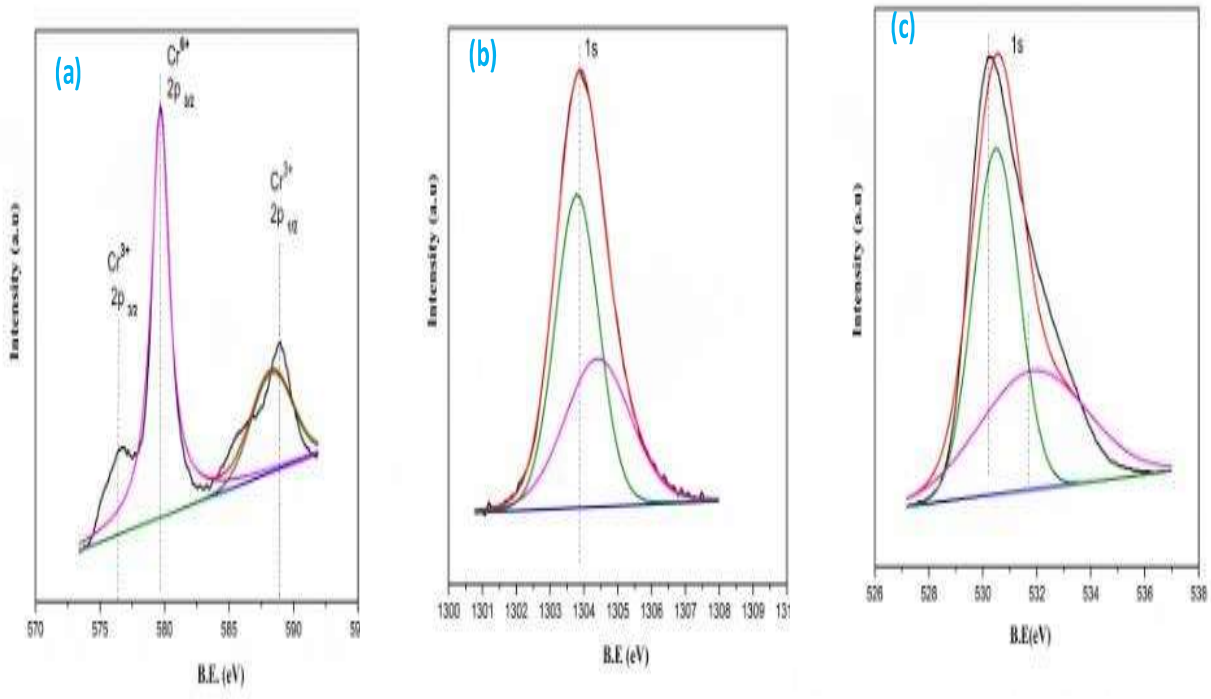

Fig 6. 5. XPS spectra of $MgCr_2O_4$ (a) 3p spectrum of chromium ion, (b) 1s spectrum of Mg^{2+} ion, (c) 1s spectrum of oxygen

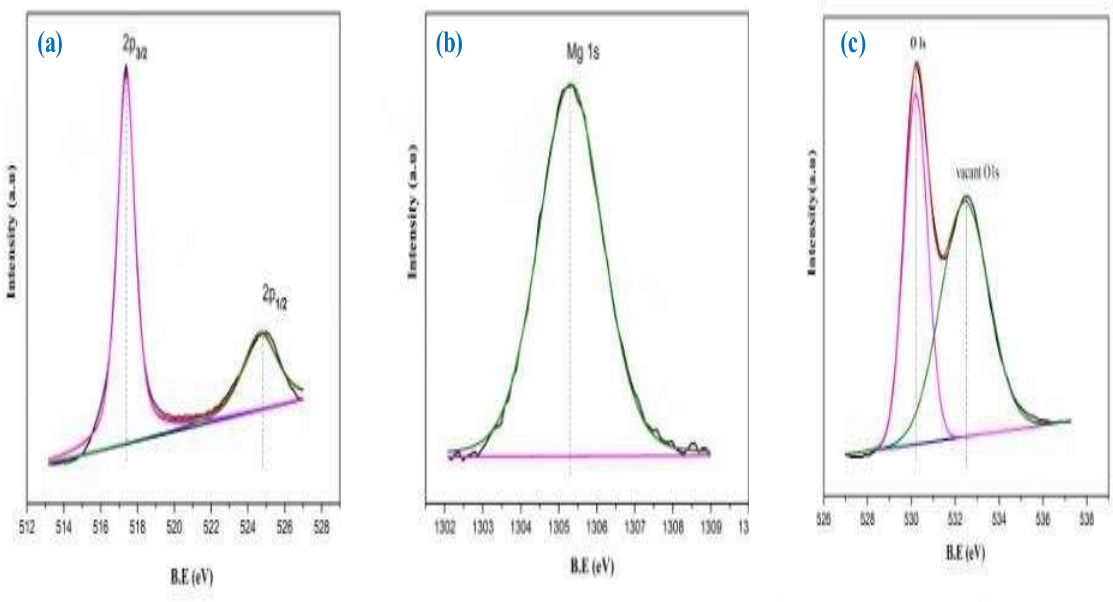

Fig 6.6. XPS spectra of MgV_2O_4 (a) 2p spectrum of Vanadium ion, (b) 1s spectrum of Mg^{2+} ion, (c) 1s spectrum of oxygen

6.4 Evaluation of catalyst for glycerol carbonate synthesis

The activity of all the prepared catalysts were tested in transesterification of glycerol-to-glycerol carbonate by simple reflux condensation process. The reaction was carried out in two different 200 ml round bottom flask taking 5.4mmol of glycerol (5g), 16.2mmol of DMC (14.6g) each followed by addition of catalysts like $MgCr_2O_4$, MgV_2O_4 separately varying the weight percentage from 1 to 10 wt.% each according to the weight of glycerol used. Subsequently the reaction mixtures were heated to attain optimum temperature for optimum time with continuous stirring. The advancement of the reactions was monitored by gas chromatography. After completion of reaction process the product mixtures were filtered for easy separation of catalyst and further study in next reaction process. The remaining DMC and methanol present in liquid mixture were also separated using rotary evaporator. The product was detected using gas chromatography (Agilent technology 7890B) equipped with flame ionization detector and capillary column HP-5 (30m ×

0.32mm × 0.25mm). Tertiary butanol was used as internal standard for quantification analysis. The conversion and yield percentage of glycerol and glycerol carbonate were calculated using the following equations. Similarly, ^{1}H and ^{13}C NMR spectra of synthesized glycerol carbonate were studied by NMR spectroscopy.

After separation of catalyst from the reaction mixture the by-product methanol obtained was evaporated by rotary evaporator and the synthesized glycerol carbonate undergoes for proton as well as carbon-13 analysis using Bruker Ascend TM 500MHz spectrometer. Dimethyl Sulfoxide–d_6 was used as a solvent and internal reference. The proton NMR spectra of synthesized glycerol carbonate is shown in fig 6.7 (a) and found to be different types of multiplet peaks at different chemical shift values responsible for protons present in the compound. The multiplet peak of chemical shift value of 4.81 ppm is mainly responsible for obtaining the conversion percentage of glycerol-to-glycerol carbonate and can be calculated by the integration area of proton NMR signal at chemical shift of 4.81ppm for methine proton of glycerol carbonate and integration area value for chemical shift of 3.43ppm for methine proton(-CH-) of glycerol. From the figure 6.7(b) shown for ^{13} C spectra of glycerol carbonate it was observed that there were four characteristic peaks of glycerol carbonate due to presence of four different carbon atoms, the peak at 155.55ppm corresponded to carbonate carbon peak of glycerol carbonate including this other three peaks were also observed at 77.60ppm,61.80ppm and 66.28ppm for C_2,C_3 and C_4carbon atoms respectively . Another multiplet peak around 40ppm was observed mainly due to the solvent dimethyl sulfoxide.

$$\text{Glycerol Conversion (\%)} = \frac{No\ of\ moles\ of\ glycerol\ reacted}{Total\ no\ of\ moles\ of\ glycerol\ taken} \times 100 \qquad (6.2)$$

$$\text{Selectivity (\%)} = \frac{No\ of\ moles\ of\ desired\ product}{Total\ no\ of\ moles\ of\ all\ products} \times 100 \qquad (6.3)$$

$$\text{Yield (\%)} = \frac{\%\ glycerol\ conv \times \%\ GLC\ selectivity}{100} \qquad (6.4)$$

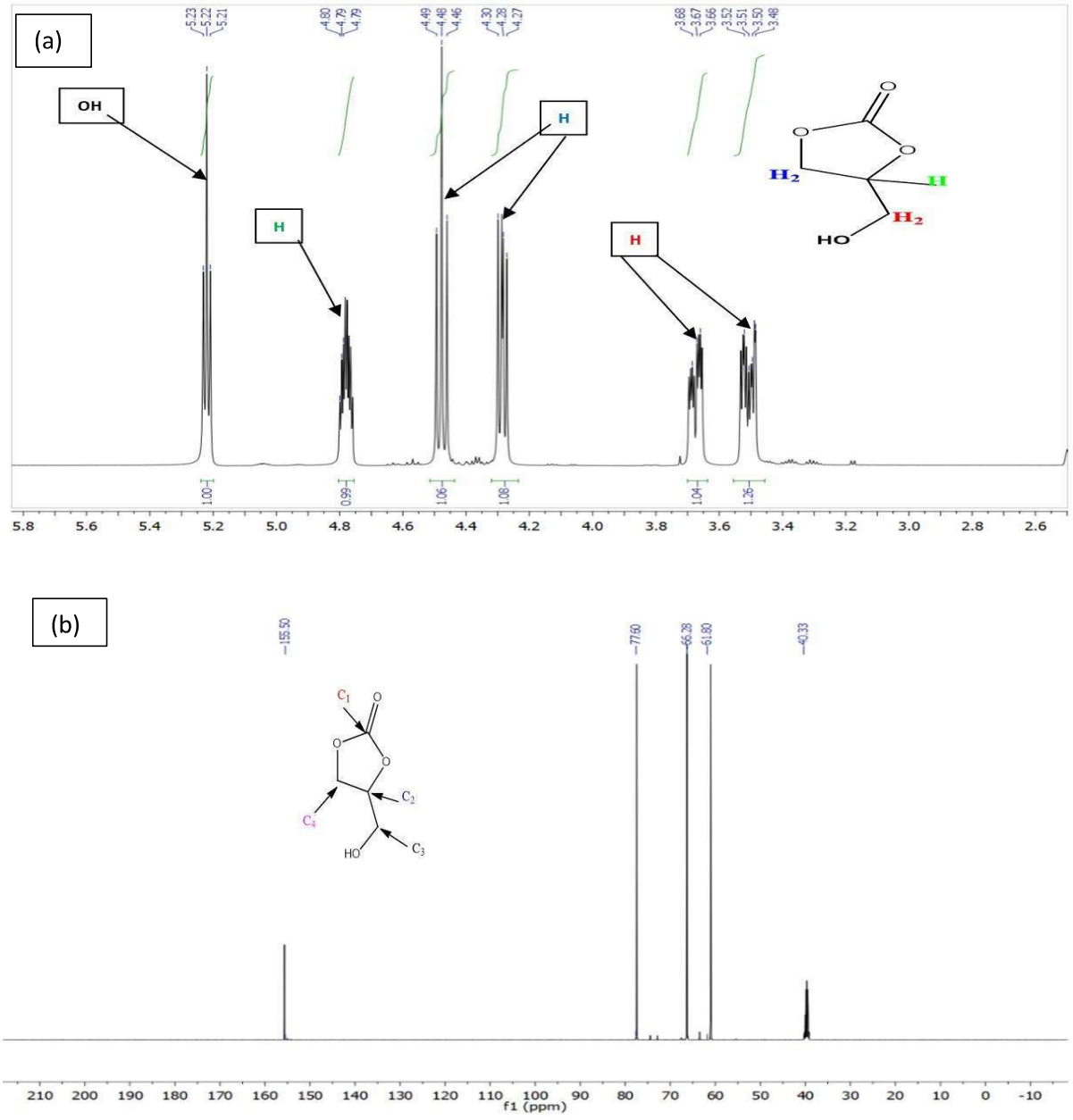

Fig 6.7 (a) ^{1}H NMR spectra, (b) ^{13}C NMR spectra of synthesized glycerol carbonate

6.5 Detailed study of reaction mechanism in transesterification of glycerol

A possible reaction pathway involved in transesterification of glycerol is depicted in fig 6.8. Initially the Lewis basic site (Mg^{2+}) of synthesized MCO catalyst abstract the acidic proton of primary hydroxyl group of glycerol with simultaneous activation of carbonyl carbon of DMC by Lewis acidic site (Cr^{3+}). As a result, the formed glyceroxide anion undergoes nucleophilic addition with activated DMC to form hydroxyl alkyl carbonate with elimination of methanol as side product. The hydroxyl alkyl carbonate being unstable intermediate undergoes cyclization to form cyclic glycerol carbonate and regenerates the catalyst. Generally, the solid base catalyst acts as a very good support for the abstraction of H^+ from glycerol by the basic site of catalyst. Higher basicity of catalyst can enhanced the more negative charge on glyceroxide anion and subsequently lower the free energy of reaction [203–205] .The designed $MgCr_2O_4$ having highest basicity promotes conversion of glycerol with highest glycerol carbonate yield of 95.7% .

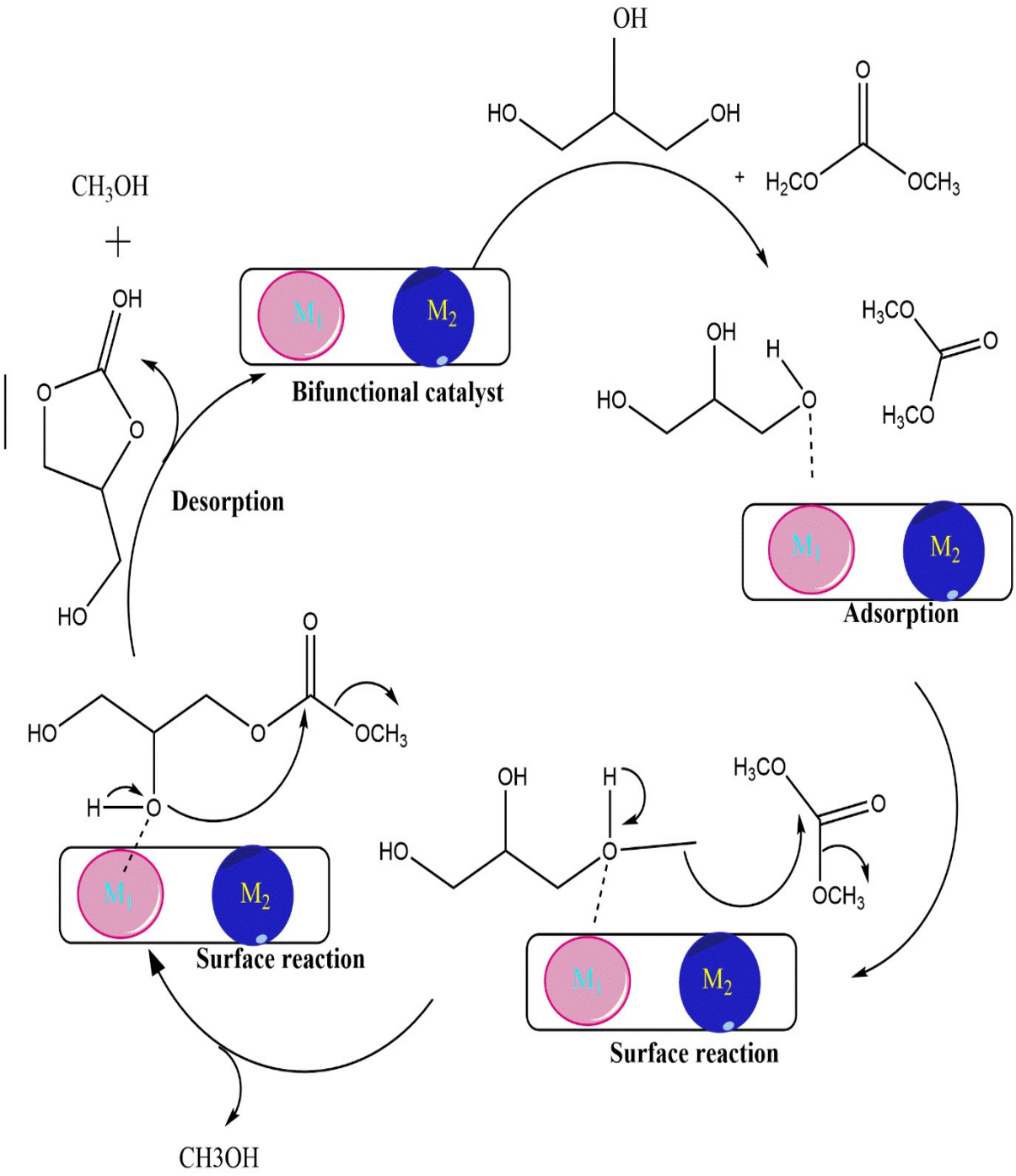

Fig 6.8. Reaction mechanism of transesterification of glycerol on MCO and MVO spinels, M_1 basic site and M_2 acidic active site.

6.6 Optimization of reaction parameters

6.6.1 Effect of reaction temperature

Temperature being one of the important parameters in transesterification of glycerol was optimized and revealed in fig 6.9 (a). It was noticed that the maximum conversion of glycerol i.e., 99.2 % was achieved at 85°C with highest GLC yield of 95.7%. There was no appreciable improvement of conversion of glycerol beyond 85°C,suggesting the decarboxylation reaction at high temperature to glycidol which further converted to polyglycerol by ring -opening polymerization [70,103]. High temperature also aggravated undesired reactions like dehydrogenation and condensation reactions of by product methanol which also reduced the activity of catalyst in conversion process of glycerol.

6.6.2 Effect of reaction time

The effect of reaction time over transesterification of glycerol was studied and shown in fig 6.9 (b). It was revealed that the reaction achieved highest conversion of 99.2 % with subsequent increase in reaction time from 20 min to 80 min. The conversion of glycerol increased from 52% to 99.2% at 80 min. The conversion as well as yield of glycerol and GLC decreased gradually when the time prolonged above 80 min, implying the conversion of glycerol carbonate to glycidol. This type of disorder in GLC yield and glycerol conversion might be due to that the reaction acquired equilibrium within 80 min [61,63] . Depending upon the product purity and energy consumption 80 min was considered to be optimum reaction time for transesterification of glycerol using this MCO catalyst.

6.6.3 Effect of DMC to glycerol molar ratio

The transesterification reaction was highly affected by molar ratio of reactants and was shown in fig 6.9 (c). It was observed that with increase in molar ratio DMC/glycerol from 1:1 to 4:1, the conversion percentage of glycerol increased from 56 to 99.2% and yield percentage of glycerol carbonate also maximized from 48 to 95.7%. Further increase of DMC to glycerol ratio above 4:1 there was gradual decrease of conversion of glycerol which might be due to immiscibility of hydrophilic glycerol and hydrophobic DMC at high concentrations i.e., solubility effect. Another phenomenon which hampered the conversion of glycerol at high DMC: glycerol molar ratio is that the rate of reaction became slower due to very low concentration of glycerol [206].

6.6.4 Effect of catalyst loading

The effect of catalyst amount used in glycerol transesterification reaction was investigated and has been depicted in fig 6. 9 (d). There was steady increase of conversion of glycerol from 62% to 99.2% with increase in catalyst amount up to 5wt% of glycerol used in reaction process. Such type of improvement in conversion percentage of glycerol might be due to increase in overall basic site of catalysts. Further increase in catalyst amount above 5wt%, the conversion of glycerol was not improved suggesting the stability of catalyst against the possible emulsification of solid-liquid mixture. Another factor that at higher catalyst masses there might be possibility of blocking of pores and lack of availability of active sites due to agglomeration of particles [204].

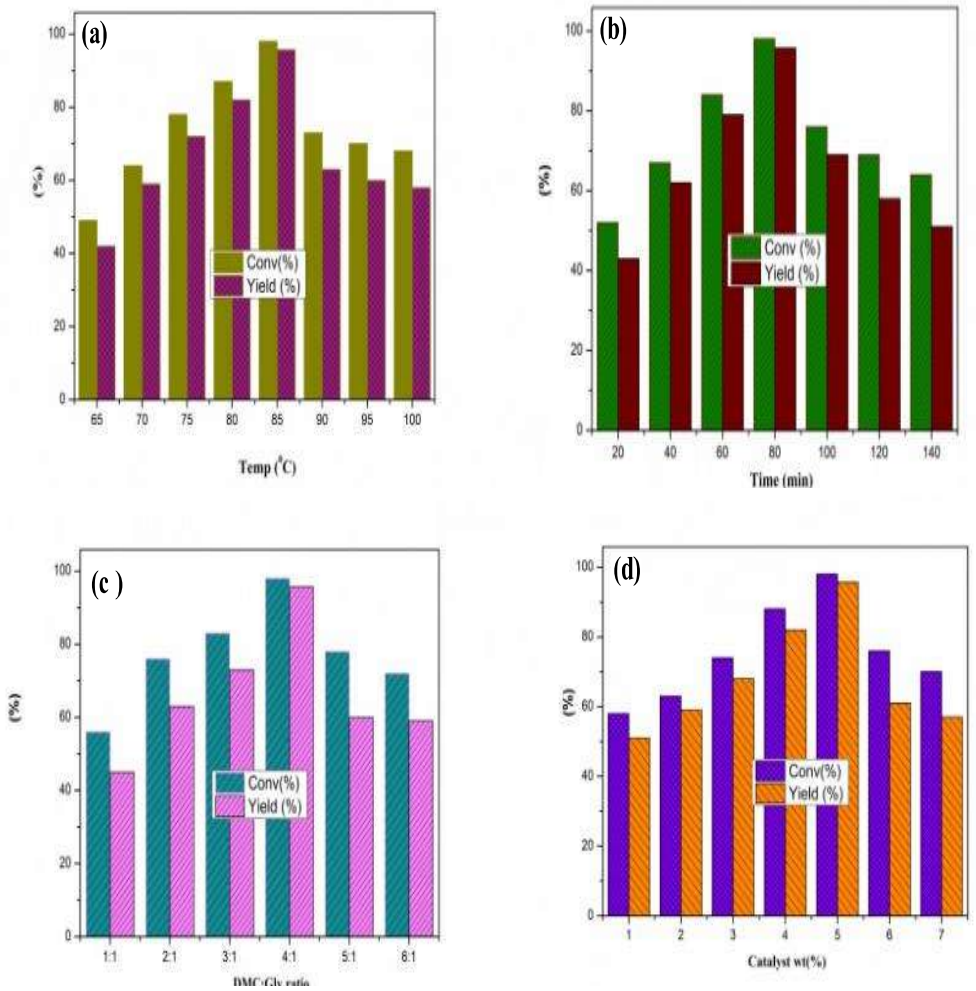

Fig 6.9. Optimization of reaction parameters catalysed by $MgCr_2O_4$ catalyst like (a) Temp, (b) Time, (c) DMC: Gly molar ratio, (d) Catalyst wt % on the basis of glycerol used.

6.6.5 Reusability of catalyst

Considering the positive effect on environment and economic factor, the stability, activity and reusability of synthesized catalyst was studied and depicted in fig 6.10. It was found that the catalyst was stable up to six cycles in transesterification of glycerol. The reusability of catalyst was investigated by leaching test through hot filtration method. In this process consecutive batch experiments were carried out and after each reaction, the catalysts were regenerated by washing thoroughly with methanol and dried in oven. Fig 6. 10 depicted the conversion percentage of glycerol and yield percentage of GLC obtained from successive

regenerated catalysts. The result revealed that the catalyst is highly efficient and reusable up to six runs with no appreciable loss of activity. The phenomenon of stability of catalyst up to 6th runs was attributed to well organized crystallite structure of its phase which helps in stabilizing the metallic species of Mg^{2+} and Cr^{3+} as confirmed by leaching test. In order to get a concrete idea related to the stability and activity of synthesized catalyst, we have also explored the physicochemical properties by XRD and SEM-EDX study and depicted in fig 6.11. From X-ray diffraction study, we obtained complete change of single phase of MCO to multiple phases of diffraction peaks after six time runs in transesterification reaction. The diffraction patterns at 2θ value 19.91°, 35.43°, 49.06° indexed to (003), (101) and (015) respectively correspond to $HCrO_2$ having rhombohedral symmetry, matched with standard pattern of JCPDS -898249. Similarly, many other diffracted peaks of Cr $(CO)_6$ also appeared with 2θ = 17.78°, (110), 20.58°, (201) 36.24° (331) which were matched with standard pattern – 720049 having orthorhombic crystal symmetry. There were peaks of $MgCO_3$ appeared due to trapping of atmospheric CO_2 by the synthesized MCO during reaction process which was also matched with JCPD file -862344. Many other peaks at 2θ= 34.54°, 51.78°, 68.82° with corresponding miller indices values (024), (113) and (404) ascribed to $Mg_6Cr_2CO_3(OH)_{16}.4H_2O$ of rhombohedral symmetry (JCPDS File- 451475). The change in crystalline structure and appearance of multiple phases disturbs the stability and activity of single phase MCO spinel after six runs. The SEM image of MCO after six time run in glycerol transesterification reaction is depicted in fig 6.11 (b). It was revealed that the particles are agglomerated and possessed irregular geometry due to presence of variable forms like Mg $(CO)_3$, Cr $(CO)_6$, $HCrO_2$ etc which highly deactivate the catalyst's active sites. Thus, the designed catalyst can be immensely endorsed to commercialize for industrial scale production of glycerol carbonate.

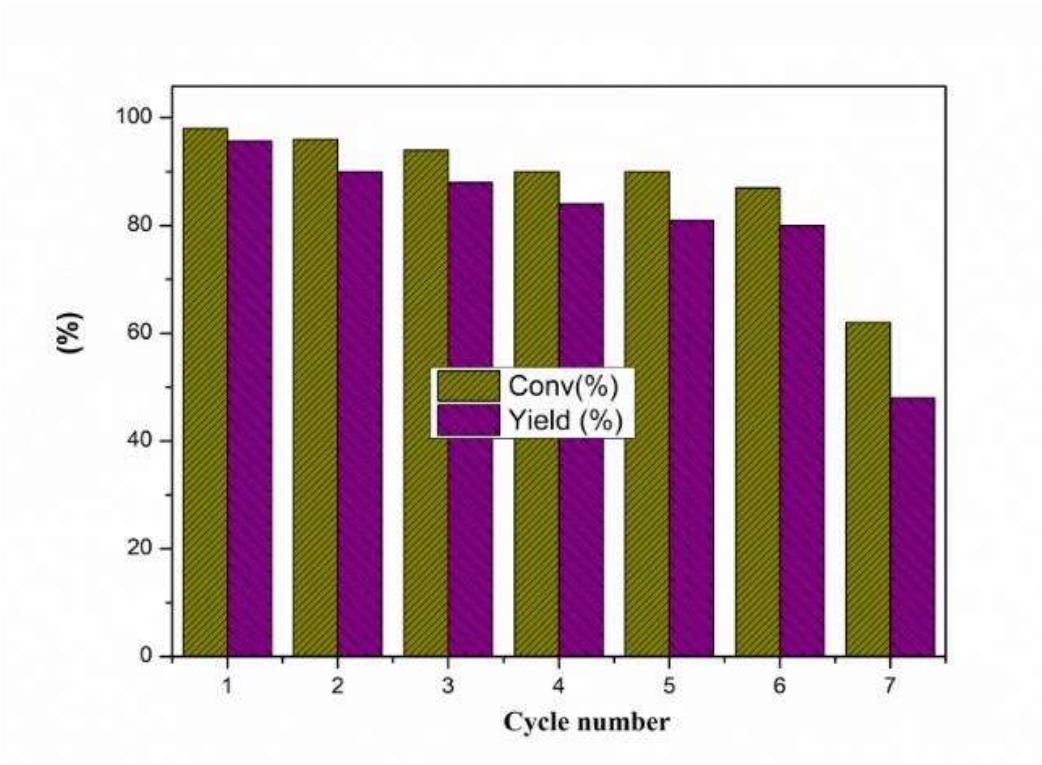

Fig 6.10. Reusability study of $MgCr_2O_4$ catalyst at optimized condition.

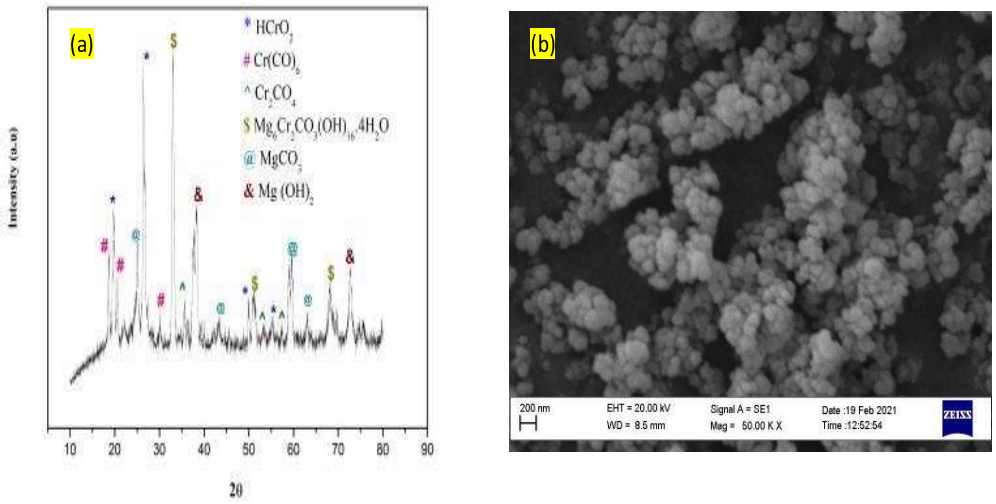

Fig 6.11.(a) XRD pattern of sixth reused MCO, (b) SEM-micrograph of sixth reused MCO.

6.7 Conclusion

In this work, a greener route was adopted for synthesis of glycerol carbonate from biowaste glycerol derived from biodiesel industries via transesterification reaction. We successfully synthesized spinels like MCO and MVO and studied the catalytic activity in transesterification of glycerol. A comparative study between spinel like MCO and MVO for transesterification reaction was conducted. The sophisticated techniques like XRD, SEM-EDX, XPS, BET - surface area, TGA revealed the complete formation of MCO and MVO framework. All the characterizations suggested that MCO possess higher basic strength, higher specific surface area, bigger lattice distortion, smaller particle size than that of MVO catalyst. All these properties of MCO were highly beneficial for conversion of glycerol-to-glycerol carbonate. Another major reason for better conversion of glycerol using MCO was that the presence of Chromium in +6 oxidation may contribute to the regulation of [O_{ads}/ O_{Lat}] ratio which enhanced the catalytic activity for glycerol transesterification relative to MVO. Various reaction parameters were optimized for better yield of glycerol carbonate and also achieved at optimized conditions.